Maximum Height Selection Scheme for Rank-3 OSM in Closed-loop MIMO Systems

[1]Changick Song, [2]Chang-Kyoo Jung, [*3]Subin Eom
[1,] *Department of Information and Communications Engineering, Korea National University of Transportation, Chungju, Korea*
c.song@ut.ac.kr
[2,] *Department of Information and Communications Engineering, Korea National University of Transportation, Chungju, Korea*
ckjung@ut.ac.kr
[3,] *School of Electrical Engineering, Korea University, Seoul, Korea*
esb777@korea.ac.kr

Abstract

Orthogonalized spatial multiplexing (OSM) scheme for multiple-input multiple-output channels has been originally developed for transmitting two data streams, which allows simple maximum likelihood decoding at the receiver with small feedback information. Recently, by extending the existing OSM scheme, a new spatial multiplexing system which supports three number of data streams was developed. In this paper, we show that the performance of the rank-3 OSM can further be improved by applying the maximum height selection (MHS) method which maximizes the minimum Euclidean distance between symbols. Through the numerical results, we show that the proposed MHS scheme outperforms the conventional OSM as well as the singular value decomposition based scheme while the computational complexity and the feedback overhead are reduced.

***Keywords**: MIMO, Closed-loop, OSM, Limited Feedback, Selection Scheme*

1. Introduction

Multiple-input multiple-output (MIMO) wireless systems have been known to obtain significant gains over single-input single-output (SISO) systems [1] [2]. The expected benefits include a spatial multiplexing (SM) gain and a diversity gain. Especially, the SM gain enables extremely high spectral efficiency by transmitting independent data streams simultaneously through multiple transmit antennas.

To achieve the potential of multiple antennas, we need full knowledge of the channel state information (CSI) at the transmitter for customizing the precoder to current channel conditions. Assuming the full CSI at the transmitter, many studies have adopted the singular value decomposition (SVD) based methods [3]–[5], which decomposes an MIMO channel into several independent eigen subchannels, and allocate resources such as power and bits over these subchannels. In time-division duplex (TDD) systems, the full CSI may be obtained using the channel reciprocity. However, in frequency-division duplex (FDD) cases, the CSI must be conveyed through a feedback channel, which is quite impractical due to the large number of channel coefficients that need to be quantized and even under flat-fading MIMO channels.

To solve the problem, orthogonalized spatial multiplexing (OSM) has been developed in [6], which allows us to simplify the maximum likelihood detection (MLD) at the receiver with small feedback information. This scheme achieves orthogonality of the channel by applying a simple rotation at the transmitter [4] [5]. In [7], an enhanced OSM (E-OSM) precoder was developed to further improve the performance. However, the conventional OSM [6] [7] was limited only to the cases of two data streams,

* Corresponding Author
Received: Jun. 11, 2015, Revised Jul. 21, Accepted: Oct. 03, 2015

which may be a problem in practice for achieving high spectral efficiency. To solve the problem, [8] proposed rank-3 OSM (ROSM) scheme that can support three number of data streams by adopting three successive rotation precoding. Then, it is shown that the complexity of the MLD at the receiver can be reduced from $O(M^3)$ to $O(M^{3/2})$ while achieving the better performance than the SVD schemes.

In this paper, we propose an enhanced ROSM (E-ROSM) scheme that further improves the performance of ROSM scheme by employing additional precoders which maximize the minimum Euclidean distance $d_{\min}$ with extra feedback information. By applying the E-ROSM precoder, it is shown that we obtain about 8dB and 5dB gains over the OSM case at a bit error rate (BER) of 10^{-4} for 4-QAM and 16-QAM, respectively without affecting the MLD complexity order at the receiver.

Throughout this paper, normal letters represent scalar quantities, boldface letters indicate vectors and boldface uppercase letters designate matrices. With a bar accounting for complex variables, for any complex notation $\bar{c}$, we denote the real and imaginary part of $\bar{c}$ by $\Re[\bar{c}]$ and $\Im[\bar{c}]$, respectively.

2. System model

We consider a spatial multiplexing scheme for closed-loop MIMO systems with M_t transmit and M_r receive antennas in a frequency flat fading channels. It is assumed that both transmitter and receiver have perfect CSI. As shown in Figure 1, at the transmitter the information bit stream is mapped to symbols to yield the M-dimensional symbol vector $\bar{\mathbf{s}} = [\bar{s}_1, \cdots, \bar{s}_M]^T$, where $[\cdot]^T$ indicates the transpose of a vector or matrix. Here M represents the number of streams to be transmitted. The M_t by M precoding matrix $\bar{\mathbf{F}}$ receives the symbol vector $\bar{\mathbf{s}}$ to generate the linearly precoded signal vector $\bar{\mathbf{x}}$ of length M_t as

$$\bar{\mathbf{x}} = \bar{\mathbf{F}}\bar{\mathbf{s}}$$

We assume that $\mathrm{Tr}(\bar{\mathbf{F}}^{\dagger}\bar{\mathbf{F}}) = M$, where $\mathrm{Tr}(\cdot)$ indicates the trace of a matrix, and $(\cdot)^{\dagger}$ denotes the complex conjugate transpose of a vector or matrix. The SNR ρ is defined as

$$\rho = \frac{E[\bar{\mathbf{s}}^{\dagger}\bar{\mathbf{F}}^{\dagger}\bar{\mathbf{F}}\bar{\mathbf{s}}]}{\sigma_n^2} = \frac{\sigma_s^2}{\sigma_n^2}\mathrm{Tr}(\bar{\mathbf{F}}^{\dagger}\bar{\mathbf{F}}) = \frac{\sigma_s^2}{\sigma_n^2}M$$

where $E[\cdot]$ accounts for expectation and σ_s^2 and σ_n^2 stand for the symbol energy and noise variance, respectively.

At the receiver side, the complex received signal vector $\bar{\mathbf{y}}$ is given by

$$\bar{\mathbf{y}} = \bar{\mathbf{H}}\bar{\mathbf{x}} + \bar{\mathbf{n}} \qquad (1)$$

where $\bar{\mathbf{n}}$ is a complex Gaussian noise vector with covariance matrix $\sigma_n^2\mathbf{I}_{M_r}$, and $\mathbf{I}_d$ indicates an identity matrix of size d .

Here the M_r by M_t channel response matrix can be written as

$$\bar{\mathbf{H}} = \begin{bmatrix} \bar{h}_{11} & \cdots & \bar{h}_{1M_t} \\ \vdots & \ddots & \vdots \\ \bar{h}_{M_r1} & \cdots & \bar{h}_{M_rM_t} \end{bmatrix} = \begin{bmatrix} \bar{\mathbf{h}}_1 & \cdots & \bar{\mathbf{h}}_{M_t} \end{bmatrix}$$

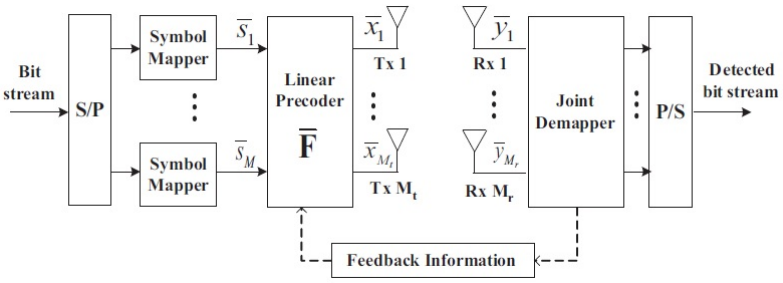

Figure 1. Schematic diagram of a closed-loop spatial multiplexing scheme with M_t transmit and M_r receive antennas

where $\bar{h}_{ji}$ represents the channel response between the i-th transmit and the j-th receive antenna, and $\bar{\mathbf{h}}_i$ denotes the i-th column vector of $\bar{\mathbf{H}}$. The whole elements of the MIMO channel matrix $\bar{\mathbf{H}}$ are obtained from an independent and identically distributed (i.i.d.) complex Gaussian distribution.

3. Conventional rank-3 OSM transmission scheme

In what follows, we give a brief review of the ROSM transmission scheme [8], which supports three independent data streams. To simplify the presentation, we focus on $M_t = M = 3.$, but we note that the scheme can be applied to all cases of $M_t > 3$. Let Q denote a QAM signal constellation of size M_c. Given the channel matrix $\bar{\mathbf{H}}$ without precoding, the ML estimate of the transmitted vector $\bar{\mathbf{x}}$ is given by

$$\hat{\bar{\mathbf{x}}} = \arg\min_{\bar{\mathbf{x}} \in Q^3} \left\| \bar{\mathbf{y}} - \bar{\mathbf{H}}\bar{\mathbf{x}} \right\|^2 \qquad (2)$$

where $\|\cdot\|$ denotes the Euclidean norm. Note that the searching size for the ML estimate exponentially increases as the number of constellation points grows.

Equivalently, the real-valued representation of the system (1) can be written as [6]

$$\mathbf{y} = \begin{bmatrix} \Re[\bar{\mathbf{y}}] \\ \Im[\bar{\mathbf{y}}] \end{bmatrix} = \mathbf{H}\mathbf{x} + \mathbf{n} \qquad (3)$$

where $\mathbf{x} = \left[\Re\left[\bar{\mathbf{x}}^T\right] \quad \Im\left[\bar{\mathbf{x}}^T\right] \right]^T$, $\mathbf{n} = \left[\Re\left[\bar{\mathbf{n}}^T\right] \quad \Im\left[\bar{\mathbf{n}}^T\right] \right]^T$, and $\mathbf{H}$ is represented by

$$\mathbf{H} = \begin{bmatrix} \Re[\bar{\mathbf{H}}] & -\Im[\bar{\mathbf{H}}] \\ \Im[\bar{\mathbf{H}}] & \Re[\bar{\mathbf{H}}] \end{bmatrix} = \left[\mathbf{h}_1 \quad \mathbf{h}_2 \quad \mathbf{h}_3 \quad \mathbf{h}_4 \quad \mathbf{h}_5 \quad \mathbf{h}_6 \right]. \qquad (4)$$

Here $\mathbf{h}_i$ denotes the i-th $2M_r$ - dimensional column vector of the real-valued channel matrix **H.**

From the real-valued representation of the channel matrix in (4), it is easy to see that the column vectors $\mathbf{h}_1$, $\mathbf{h}_2$ and $\mathbf{h}_3$ are orthogonal to $\mathbf{h}_4$, $\mathbf{h}_5$ and $\mathbf{h}_6$, respectively (i.e., $\mathbf{h}_1 \perp \mathbf{h}_4$, $\mathbf{h}_2 \perp \mathbf{h}_5$ and $\mathbf{h}_3 \perp \mathbf{h}_6$). We also note that column vectors $\mathbf{h}_1$, $\mathbf{h}_2$ and $\mathbf{h}_3$ share the same property with $\mathbf{h}_4$, $\mathbf{h}_5$ and $\mathbf{h}_6$. In other words, $\|\mathbf{h}_1\| = \|\mathbf{h}_4\|$, $\|\mathbf{h}_2\| = \|\mathbf{h}_5\|$, $\|\mathbf{h}_3\| = \|\mathbf{h}_6\|$, and the angles between each pair of vectors are the same as those between the corresponding vectors (i.e., $\bar{\mathbf{h}}_i^T \bar{\mathbf{h}}_j = \bar{\mathbf{h}}_{i+3}^T \bar{\mathbf{h}}_{j+3}$ for $i \neq j$). These properties do not change with the subsequent precoding process.

Note that the ML detection in (3) requires $O\left(M_c^3\right)$. Now, we present the ROSM precoder to simplify the MLD. To achieve this goal, we encode the three transmitted symbols as

$$\bar{\mathbf{x}} = \bar{\mathbf{F}}_\theta \bar{\mathbf{s}}, \qquad (5)$$

where $\bar{\mathbf{F}}_\theta$ accounts for the orthogonalizing precoding matrix. The system model in (1) then becomes

$$\bar{\mathbf{y}} = \bar{\mathbf{H}}\bar{\mathbf{F}}_\theta \bar{\mathbf{s}} + \bar{\mathbf{n}} = \bar{\mathbf{H}}_\theta \bar{\mathbf{s}} + \bar{\mathbf{n}}. \quad (6)$$

Define the effective channel $\bar{\mathbf{H}}_\theta \triangleq \bar{\mathbf{H}}\bar{\mathbf{F}}_\theta = \left[\bar{\mathbf{h}}_1^\theta \quad \bar{\mathbf{h}}_2^\theta \quad \bar{\mathbf{h}}_3^\theta\right]$. Then the real valued representation of the effective matrix is equivalently denoted by $\mathbf{H}_\theta$ as

$$\mathbf{H}_\theta = \left[\mathbf{h}_1^\theta \quad \mathbf{h}_2^\theta \quad \mathbf{h}_3^\theta \quad \mathbf{h}_4^\theta \quad \mathbf{h}_5^\theta \quad \mathbf{h}_6^\theta\right], \quad (7)$$

where $\bar{\mathbf{h}}_i^\theta$ and $\mathbf{h}_i^\theta$ denote the i-th column of matrix, the precoding matrix $\bar{\mathbf{F}}_\theta$ in (7) is composed of three successive processing as $\bar{\mathbf{F}}_\theta = \bar{\mathbf{F}}_1\bar{\mathbf{F}}_2\bar{\mathbf{F}}_3$, where

$$\bar{\mathbf{F}}_1 = \begin{bmatrix} e^{j\theta_1} & 0 & 0 \\ 0 & 1 & 0 \\ 0 & 0 & 1 \end{bmatrix}, \bar{\mathbf{F}}_2 = \begin{bmatrix} \cos\theta_2 & -\sin\theta_2 & 0 \\ \sin\theta_2 & \cos\theta_2 & 0 \\ 0 & 0 & 1 \end{bmatrix} \text{ and } \bar{\mathbf{F}}_3 = \begin{bmatrix} e^{j\theta_3} & 0 & 0 \\ 0 & e^{j\theta_4} & 0 \\ 0 & 0 & 1 \end{bmatrix}. \quad (8)$$

Consequently, we can obtain $\bar{\mathbf{F}}_\theta$ as

$$\bar{\mathbf{F}}_\theta = \begin{bmatrix} \cos\theta_2 e^{j(\theta_1+\theta_3)} & -\sin\theta_2 e^{j(\theta_1+\theta_4)} & 0 \\ \sin\theta_2 e^{j\theta_3} & \cos\theta_2 e^{j\theta_4} & 0 \\ 0 & 0 & 1 \end{bmatrix}. \quad (9)$$

Here we define $\bar{\mathbf{H}}_{\theta_1} \triangleq \bar{\mathbf{H}}\bar{\mathbf{F}}_1$ and $\bar{\mathbf{H}}_{\theta_2} \triangleq \bar{\mathbf{H}}\bar{\mathbf{F}}_1\bar{\mathbf{F}}_2$. Recall that the column vectors $\mathbf{h}_1$, $\mathbf{h}_2$ and $\mathbf{h}_3$ are orthogonal to $\mathbf{h}_4$, $\mathbf{h}_5$ and $\mathbf{h}_6$, respectively. First, let us consider four vectors $\mathbf{h}_1$, $\mathbf{h}_2$, $\mathbf{h}_4$ and $\mathbf{h}_5$. Denoting span(**u**,**v**) as the subspace spanned by **u** and **v**, we can allocate these four vectors in two orthogonal subspaces span($\mathbf{h}_1^{\theta_1}, \mathbf{h}_2^{\theta_1}$) and span($\mathbf{h}_4^{\theta_1}, \mathbf{h}_5^{\theta_1}$) only if we have $\mathbf{h}_1^{\theta_1} \perp \mathbf{h}_5^{\theta_1}$ and $\mathbf{h}_2^{\theta_1} \perp \mathbf{h}_4^{\theta_1}$, since $\mathbf{h}_1, \mathbf{h}_4$ and $\mathbf{h}_2, \mathbf{h}_5$ are already orthogonal to each other, regardless of θ_1. We obtain

$$\mathbf{h}_1^{\theta_1} \cdot \mathbf{h}_5^{\theta_1} = \left(\mathbf{h}_1 \cos\theta_1 + \mathbf{h}_5 \sin\theta_1\right) \cdot \mathbf{h}_5, \quad (10)$$

where $\mathbf{h}_i \cdot \mathbf{h}_j$ denotes the inner (dot) product between vectors $\mathbf{h}_i$ and $\mathbf{h}_j$. Since $\mathbf{h}_2^{\theta_1} \cdot \mathbf{h}_4^{\theta_1} = -\mathbf{h}_1^{\theta_1} \cdot \mathbf{h}_5^{\theta_1}$, the orthogonality can be achieved when $\mathbf{h}_1^{\theta_1} \cdot \mathbf{h}_5^{\theta_1}$ in (10) becomes zero. After some manipulations, θ_1 can be computed as [6]

$$\theta_1 = \tan^{-1}\left(\frac{\omega_B}{\omega_A}\right) \quad (11)$$

where $\omega_A = \mathbf{h}_4^T\mathbf{h}_5$, and $\omega_B = -\mathbf{h}_1^T\mathbf{h}_5$

Next, the orthogonality between $\mathbf{h}_1^{\theta_1}$ and $\mathbf{h}_2^{\theta_1}$ is easily achieved by a precoder $\bar{\mathbf{F}}_2$ if the inner product of $\mathbf{h}_1^{\theta_2}$ and $\mathbf{h}_2^{\theta_2}$ becomes zero as

$$\left(\mathbf{h}_1^{\theta_2}\right)^T \mathbf{h}_2^{\theta_2} = \left(\left\|\mathbf{h}_2^{\theta_1}\right\|^2 - \left\|\mathbf{h}_1^{\theta_1}\right\|^2\right)\cos\theta_2 \sin\theta_2 + \left(\cos^2\theta_2 - \sin^2\theta_2\right)\left(\mathbf{h}_1^{\theta_1}\right)^T \mathbf{h}_2^{\theta_1} = 0. \quad (12)$$

Note that the rotation processing $\mathbf{F}_2$ does not have any effects on the orthogonality between two subspaces. Solving equation (12) with respect to θ_2 yields the rotation angle

$$\theta_2 = \tan^{-1}\left(\frac{\omega_C \pm \sqrt{\omega_C^2 + 4\omega_D^2}}{2\omega_D}\right)$$

where $\omega_C = \left\|\mathbf{h}_2^{\theta_1}\right\|^2 - \left\|\mathbf{h}_1^{\theta_1}\right\|^2$ and $\omega_D = \left(\mathbf{h}_1^{\theta_1}\right)^T \mathbf{h}_2^{\theta_1}$. Here we note that $\left\|\mathbf{h}_1^{\theta_2}\right\|$ is maximized for $\theta_2 = \tan^{-1}\left(\frac{\omega_C + \sqrt{\omega_C^2 + 4\omega_D^2}}{2\omega_D}\right)$ whereas $\left\|\mathbf{h}_2^{\theta_2}\right\|$ is maximized for $\theta_2 = \tan^{-1}\left(\frac{\omega_C - \sqrt{\omega_C^2 + 4\omega_D^2}}{2\omega_D}\right)$. Throughout this paper, we consider only the first case ($\left\|\mathbf{h}_1^{\theta_2}\right\| \geq \left\|\mathbf{h}_2^{\theta_2}\right\|$).

Until now, it has been shown that by adopting two rotation matrices $\bar{\mathbf{F}}_1$ and $\bar{\mathbf{F}}_2$, we can obtain fully orthogonalized column vectors $\mathbf{h}_1^{\theta_2}$, $\mathbf{h}_2^{\theta_2}$, $\mathbf{h}_4^{\theta_2}$ and $\mathbf{h}_5^{\theta_2}$ (i.e., $\mathbf{h}_1^{\theta_2} \perp \mathbf{h}_2^{\theta_2} \perp \mathbf{h}_4^{\theta_2} \perp \mathbf{h}_5^{\theta_2}$). Note that the

magnitude of $\mathbf{h}_1^{\theta_2}$ and $\mathbf{h}_2^{\theta_2}$ is equal to the first and the second singular values of the matrix consisting of first two columns of $\overline{\mathbf{H}}$ in (1). Since we have already orthogonalized all four vectors, additional rotation on $\mathbf{h}_1^{\theta_2}$ and $\mathbf{h}_4^{\theta_2}$, or $\mathbf{h}_2^{\theta_2}$ and $\mathbf{h}_5^{\theta_2}$ does not affect the orthogonality. Our final goal is to achieve full orthogonality

$$\text{span}\left(\mathbf{h}_1^{\theta},\mathbf{h}_2^{\theta},\mathbf{h}_3^{\theta}\right) \perp \text{span}\left(\mathbf{h}_4^{\theta},\mathbf{h}_5^{\theta},\mathbf{h}_6^{\theta}\right).$$

To this end, we employ $\mathbf{F}_3$ to have

$$\text{span}\left(\mathbf{h}_1^{\theta},\mathbf{h}_3^{\theta}\right) \perp \text{span}\left(\mathbf{h}_4^{\theta},\mathbf{h}_6^{\theta}\right).$$

and

$$\text{span}\left(\mathbf{h}_2^{\theta},\mathbf{h}_3^{\theta}\right) \perp \text{span}\left(\mathbf{h}_5^{\theta},\mathbf{h}_6^{\theta}\right).$$

As in equation (10), this is achieved by $\left(\mathbf{h}_1^{\theta}\right)^T \mathbf{h}_6^{\theta} = 0$ and $\left(\mathbf{h}_2^{\theta}\right)^T \mathbf{h}_6^{\theta} = 0$ where θ_3 and θ_4 in $\overline{\mathbf{F}}_3$ are given by

$$\theta_3 = \tan^{-1}\left(\frac{-\left(\mathbf{h}_1^{\theta_2}\right)^T \mathbf{h}_6^{\theta_2}}{\left(\mathbf{h}_4^{\theta_2}\right)^T \mathbf{h}_6^{\theta_2}}\right),\ \theta_4 = \tan^{-1}\left(\frac{-\left(\mathbf{h}_2^{\theta_2}\right)^T \mathbf{h}_6^{\theta_2}}{\left(\mathbf{h}_5^{\theta_2}\right)^T \mathbf{h}_6^{\theta_2}}\right).$$

Using these successive precoding operations, we can divide the channel into the two independent subchannels $\mathbf{H}_I \triangleq \left[\mathbf{h}_1^{\theta} \quad \mathbf{h}_2^{\theta} \quad \mathbf{h}_3^{\theta}\right]$ and $\mathbf{H}_Q \triangleq \left[\mathbf{h}_4^{\theta} \quad \mathbf{h}_5^{\theta} \quad \mathbf{h}_6^{\theta}\right]$, which have the same channel quality since $\left\|\mathbf{h}_1^{\theta}\right\| = \left\|\mathbf{h}_4^{\theta}\right\|$, $\left\|\mathbf{h}_2^{\theta}\right\| = \left\|\mathbf{h}_5^{\theta}\right\|$, $\left\|\mathbf{h}_3^{\theta}\right\| = \left\|\mathbf{h}_6^{\theta}\right\|$, and $\mathbf{h}_1^{\theta} \cdot \mathbf{h}_2^{\theta} = \mathbf{h}_4^{\theta} \cdot \mathbf{h}_5^{\theta}$, $\mathbf{h}_1^{\theta} \cdot \mathbf{h}_3^{\theta} = \mathbf{h}_4^{\theta} \cdot \mathbf{h}_6^{\theta}$, $\mathbf{h}_2^{\theta} \cdot \mathbf{h}_3^{\theta} = \mathbf{h}_5^{\theta} \cdot \mathbf{h}_6^{\theta}$. Thus, the ML solution in (2) can be individually given by

$$\hat{\mathbf{s}}_I = \arg \min_{\overline{\mathbf{s}} \in \Re[Q]^3} \left\|\mathbf{y} - \mathbf{H}_I \Re\left[\overline{\mathbf{s}}\right]\right\|^2 \qquad (13)$$

Table 1. Pairs of p and θ_2 for the 2-dimensional optimal precoding (k =A/B)

Modulation	Case	p	θ_2	$d_{\min}^2$
4-QAM	$1 \le k < 7$	$\sqrt{\frac{6}{k+3}}$	$\pi/4$	$\frac{4kB}{k+3}$
	$k \ge 7$	$\sqrt{2}$	0.464	$\frac{2kB}{5}$
16-QAM	$1 \le k < 7.59$	$\sqrt{\frac{6}{k+3}}$	$\pi/4$	$\frac{4kB}{k+3}$
	$7.59 \le k < 43.1$	$\sqrt{\frac{42}{k+21}}$	0.488	$\frac{10.8kB}{k+21}$
	$43.1 \le k < 101$	$\sqrt{\frac{182}{k+91}}$	0.345	$\frac{22.6kB}{k+91}$
	$k \ge 101$	$\sqrt{2}$	0.245	$\frac{2kB}{5}$

and

$$\hat{\mathbf{s}}_Q = \arg \min_{\overline{\mathbf{s}} \in \Im[Q]^3} \left\|\mathbf{y} - \mathbf{H}_Q \Im\left[\overline{\mathbf{s}}\right]\right\|^2, \qquad (14)$$

where $\mathbf{s}_I$ and $\mathbf{s}_Q$ stand for real-valued 3-dimensional hyper constellation symbols with dimension of $\sqrt{M_C}$. The simple ML equations in (13) and (14) guarantees considerable reduction in the decoding complexity from $O\left(M_C^M\right)$ to $O\left(M_C^{M/2}\right)$ compared to the conventional ML detection.

4. Proposed maximum height selection algorithm

In this section, we propose E-ROSM scheme, and thereby showing that a few more feedback bits can substantially improve the performance. A quantized precoding scheme which maximizes the minimum Euclidean distance $d_{\min}$ in the signal space has been developed and shown that the full diversity order $\left(M_T M_R\right)$ is achievable [7]. However the application of this scheme is still limited to the rank-2 (two symbol) transmission scheme, and thus we need to find a way to increase $d_{\min}$ in the rank-3 signal space. Note that it is not easy to find the optimal 3-dimensional rotation precoder. Therefore, we propose a near optimum precoding scheme using 2-dimensional successive rotation combined with power loading. The numerical results in Section 5 show that our approximated method achieves the full diversity order.

Let us denote P by a $d_{\min}$ maximizing precoder. Then, the received signal at the receiver can be written by

$$\overline{\mathbf{y}} = \overline{\mathbf{H}}\overline{\mathbf{F}}_\theta \mathbf{P}\overline{\mathbf{s}} + \overline{\mathbf{n}} = \overline{\mathbf{H}}_\theta \mathbf{P}\overline{\mathbf{s}} + \overline{\mathbf{n}}. \qquad (15)$$

Then its real and imaginary parts are expressed as $\Re\left[\overline{\mathbf{y}}\right] = \mathbf{H}_I \mathbf{P}\mathbf{s}_I + \Re\left[\overline{\mathbf{n}}\right]$ and $\Im\left[\overline{\mathbf{y}}\right] = \mathbf{H}_Q \mathbf{P}\mathbf{s}_Q + \Im\left[\overline{\mathbf{n}}\right]$. Here P consists of real rotation matrices $\mathbf{R}_{\theta_1}$ and $\mathbf{R}_{\theta_2}$, a real diagonal matrix D, and a permutation matrix $\mathbf{P}_M$ as $\mathbf{P} = \mathbf{P}_M \mathbf{R}_{\theta_1} \mathbf{D} \mathbf{R}_{\theta_2}$ where

$$\mathbf{R}_{\Theta_1} = \begin{bmatrix} \mathbf{R}'_{\Theta_1} & 0 \\ 0 & 1 \end{bmatrix}, \mathbf{D} = \begin{bmatrix} \mathbf{D}'_p \mathbf{D}'_q & 0 \\ 0 & q \end{bmatrix}, \text{and } \mathbf{R}_{\Theta_2} = \begin{bmatrix} \mathbf{R}'_{\Theta_2} & 0 \\ 0 & 1 \end{bmatrix}.$$

The submatrices $\mathbf{D}'_q$ and $\mathbf{D}'_p$ are represented as

$$\mathbf{D}'_q = \begin{bmatrix} \sqrt{\frac{3-q^2}{2}} & 0 \\ 0 & \sqrt{\frac{3-q^2}{2}} \end{bmatrix}, \quad \mathbf{D}'_p = \begin{bmatrix} p & 0 \\ 0 & \sqrt{2-p^2} \end{bmatrix},$$

and $\mathbf{R}'_{\Theta_1}$ and $\mathbf{R}'_{\Theta_2}$ indicate a 2 by 2 Givens rotation matrix with Θ_1 and Θ_2, respectively. Note that the additional precoder P does not change the total transmit power as

$$E\left[\operatorname{tr}\left(\overline{\mathbf{F}}_\theta \mathbf{P}\overline{\mathbf{s}\mathbf{s}}^H \mathbf{P}^H \overline{\mathbf{F}}_\theta^H\right)\right] = \sigma_s^2 \operatorname{tr}\left(\overline{\mathbf{F}}_\theta \mathbf{R}_{\Theta_1} \mathbf{D}^2 \mathbf{R}_{\Theta_1}^H \overline{\mathbf{F}}_\theta^H\right) = \operatorname{tr}\left(\mathbf{D}^2\right) = \sigma_s^2 M,$$

since $\overline{\mathbf{F}}_\theta \mathbf{R}_{\Theta_1}$ is unitary.

Now we define $\mathbf{H}_I \mathbf{P}_M \mathbf{R}_{\Theta_1}$ and $\mathbf{H}_I \mathbf{P}$ as $\mathbf{R}_d$ and $\mathbf{R}_p$, respectively. Also we refer to the j-th column of each matrix $\mathbf{R}_d$ and $\mathbf{R}_p$ as $\mathbf{r}_j^d$ and $\mathbf{r}_j^p$. For better understanding, we assume that $\mathbf{r}_1^d \perp \mathbf{r}_2^d$, $\left\|\mathbf{r}_1^d\right\| \geq \left\|\mathbf{r}_2^d\right\|$, $0 \leq \Theta_2 \leq 45^\circ$ and $U \geq 0, V \geq 0$, where $U \triangleq \left(\mathbf{r}_1^d\right)^T \mathbf{r}_3^d$ and $V \triangleq \left(\mathbf{r}_2^d\right)^T \mathbf{r}_3^d$. Let us consider first the 4-QAM modulation. Then the magnitude of real and imaginary parts of each transmitted symbol is 1/2 or -1/2. From the system model (1), the noiseless received symbols in the effective channel become $\left(\mathbf{r}_1^p + \mathbf{r}_2^p + \mathbf{r}_3^p\right)/2$, $\left(\mathbf{r}_1^p + \mathbf{r}_2^p - \mathbf{r}_3^p\right)/2$, $\left(\mathbf{r}_1^p - \mathbf{r}_2^p + \mathbf{r}_3^p\right)/2$, $\left(\mathbf{r}_1^p - \mathbf{r}_2^p - \mathbf{r}_3^p\right)/2$, $\left(-\mathbf{r}_1^p + \mathbf{r}_2^p + \mathbf{r}_3^p\right)/2$, $\left(-\mathbf{r}_1^p + \mathbf{r}_2^p - \mathbf{r}_3^p\right)/2$, $\left(-\mathbf{r}_1^p - \mathbf{r}_2^p + \mathbf{r}_3^p\right)/2$, and $\left(-\mathbf{r}_1^p - \mathbf{r}_2^p - \mathbf{r}_3^p\right)/2$. Then our goal is to maximize $d_{\min}$ between received symbols. After same manipulations, all possible Euclidean distances are listed in Table 2, where $A \triangleq \left\|\mathbf{r}_1^d\right\|^2$, $B \triangleq \left\|\mathbf{r}_2^d\right\|^2$, and $C \triangleq \left\|\mathbf{r}_3^d\right\|^2$.

First of all, we select a column vector of the channel matrix $\mathbf{H}_I$ or $\mathbf{H}_Q$ with the maximum distance from the vector space spanned by the other two vectors, where the distance Δ is defined as

$$\Delta = \left\| \left(\mathbf{I} - \mathbf{Q}\left(\mathbf{Q}^T\mathbf{Q}\right)^{-1}\mathbf{Q}^T \right)\mathbf{b} \right\|. \qquad (16)$$

Here **I** and **Q** stand for a identity matrix and a matrix whose columns span certain space, respectively, and **b** represents a vector to be projected on that space. In order to prevent confusing this newly defined distance with the Euclidean distance between received symbols, we rename the former as height. After the selection, we allocate the selected vector to the third column using the permutation matrix. Then by applying a proper value of q in $\mathbf{D}$, the minimum Euclidean distance between received symbols can be determined by only the first two columns. In that case, we can maximize $d_{\min}$ just using the 2-dimensional optimal precoder $\mathbf{D}'_p\mathbf{R}'_{\Theta_2}$ [7]. We refer to these processing as Max-Height Selection (MHS).

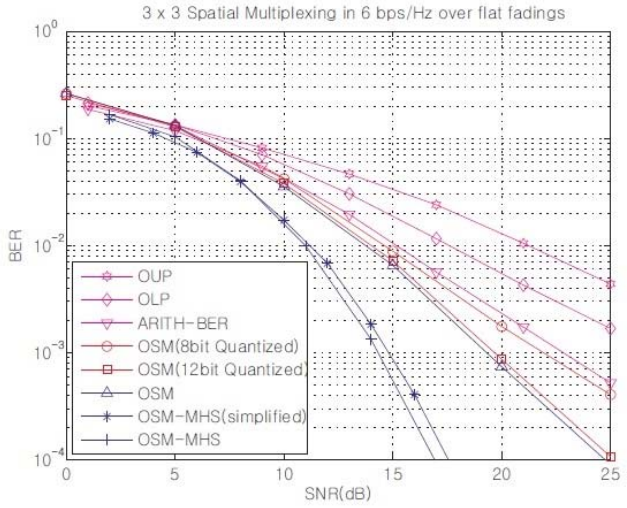

Figure 2. BER performance comparison of the proposed schemes with 4QAM

From Table 2, we can easily check that the candidates of $d_{\min}$ reduce to $\left\|\mathbf{r}_2^p\right\|$, $\left\|\mathbf{r}_3^p\right\|$, $\left\|\mathbf{r}_2^p+\mathbf{r}_3^p\right\|$, $\left\|\mathbf{r}_1^p-\mathbf{r}_3^p\right\|$, $\left\|\mathbf{r}_1^p+\mathbf{r}_2^p-\mathbf{r}_3^p\right\|$, and $\left\|\mathbf{r}_1^p-\mathbf{r}_2^p-\mathbf{r}_3^p\right\|$. Here, for simplicity we will not consider $\left\|\mathbf{r}_1^p+\mathbf{r}_2^p\right\|$, since with the optimal value of p, $\left\|\mathbf{r}_1^p+\mathbf{r}_2^p\right\|$ is exactly same as $\left\|\mathbf{r}_2^p\right\|$. Then we determine the minimum value of q, which makes all of the following matrices positive, $\left\|\mathbf{r}_3^p\right\|-\left\|\mathbf{r}_2^p\right\|$, $\left\|\mathbf{r}_2^p+\mathbf{r}_3^p\right\|-\left\|\mathbf{r}_2^p\right\|$, $\left\|\mathbf{r}_1^p-\mathbf{r}_3^p\right\|-\left\|\mathbf{r}_2^p\right\|$, $\left\|\mathbf{r}_1^p+\mathbf{r}_2^p-\mathbf{r}_3^p\right\|-\left\|\mathbf{r}_2^p\right\|$, $\left\|\mathbf{r}_1^p-\mathbf{r}_2^p-\mathbf{r}_3^p\right\|-\left\|\mathbf{r}_2^p\right\|$.

After some tedious mathematical manipulations, we can optimal value q as shown in Table 3, where W is denoted by $\max\left(pU,\left(2-p^2\right)V\right)$, and $d_{\min}$ represents the maximized minimum Euclidean distance between first two vectors of $\mathbf{H}_I$ or $\mathbf{H}_Q$ with respect to k. We can simplify the representation to reduce the computational complexity with a little performance loss. It was shown in [7] that the variation in the optimal p is small, thus we can simply replace the variable p with 1 or $\sqrt{2}$. Similarly, simulations show that the optimal value q is centered on 1 with small variance. Note that the case $q=1$ indicates no use of power loading $\mathbf{D}'_q$ (i.e., $\mathbf{D}'_q=\mathbf{I}$). Thus, only with the

information on the vector with the maximum height, we can achieve quite good performance. The approach made in this section can be extended to higher modulation systems such as 16-QAM or 64-QAM.

5. Simulation results

In this section, Monte Carlo simulations were performed to illustrate the performance of the proposed OSM precoders. In all simulations, we consider three independent data streams in the sense of high spectral efficiency. In Figure 2, we compare various systems for 4-QAM constellations. In this plot, we depict the BER performance of OUP, OLP and ARITHBER. Compared to the normal OSM, OSM-MHS additionally requires one feedback value Θ_1, one bit for rotation angle Θ_2, and two bits

	$p = \sqrt{\frac{6B}{A+3B}}$, $\Theta_2 = \frac{\pi}{4}$ $(A \le 7B)$	$p=\sqrt{2}, \Theta_2 = 0.464$ $(A \ge 7B)$
$\left\|\mathbf{r}_1^p\right\|^2$	$\left(\frac{3-q^2}{2}\right)\left(\frac{p^2A+(2-p^2)B}{2}\right)$	$0.4\left(3-q^2\right)p^2A$
$\left\|\mathbf{r}_2^p\right\|^2$	$\left(\frac{3-q^2}{2}\right)\left(\frac{p^2A+(2-p^2)B}{2}\right)$	$0.1\left(3-q^2\right)p^2A$
$\left\|\mathbf{r}_3^p\right\|^2$	q^2C	q^2C
$\left\|\mathbf{r}_1^p+\mathbf{r}_2^p\right\|^2$	$\left(3-q^2\right)\left(2-p^2\right)B$	$0.1\left(3-q^2\right)p^2A$
$\left\|\mathbf{r}_1^p-\mathbf{r}_2^p\right\|^2$	$\left(3-q^2\right)p^2A$	$0.9\left(3-q^2\right)p^2A$
$\left\|\mathbf{r}_1^p+\mathbf{r}_3^p\right\|^2$	$\left(\frac{3-q^2}{2}\right)\left(\frac{p^2A+(2-p^2)B}{2}\right)+q^2C+q\sqrt{3-q^2}\left(pU+\left(\sqrt{2-p^2}\right)V\right)$	$0.4\left(3-q^2\right)p^2A+q^2C+1.8q\sqrt{\frac{3-q^2}{2}}pU$
$\left\|\mathbf{r}_2^p+\mathbf{r}_3^p\right\|^2$	$\left(\frac{3-q^2}{2}\right)\left(\frac{p^2A+(2-p^2)B}{2}\right)+q^2C-q\sqrt{3-q^2}\left(pU-\left(\sqrt{2-p^2}\right)V\right)$	$0.1\left(3-q^2\right)p^2A+q^2C-0.9q\sqrt{\frac{3-q^2}{2}}pU$
$\left\|\mathbf{r}_1^p-\mathbf{r}_3^p\right\|^2$	$\left(\frac{3-q^2}{2}\right)\left(\frac{p^2A+(2-p^2)B}{2}\right)+q^2C-q\sqrt{3-q^2}\left(pU+\left(\sqrt{2-p^2}\right)V\right)$	$0.4\left(3-q^2\right)p^2A+q^2C-1.8q\sqrt{\frac{3-q^2}{2}}pU$
$\left\|\mathbf{r}_2^p+\mathbf{r}_3^p\right\|^2$	$\left(\frac{3-q^2}{2}\right)\left(\frac{p^2A+(2-p^2)B}{2}\right)+q^2C+q\sqrt{3-q^2}\left(pU-\left(\sqrt{2-p^2}\right)V\right)$	$0.1\left(3-q^2\right)p^2A+q^2C+0.9q\sqrt{\frac{3-q^2}{2}}pU$
$\left\|\mathbf{r}_1^p+\mathbf{r}_2^p+\mathbf{r}_3^p\right\|^2$	$\left(3-q^2\right)\left(2-p^2\right)B+q^2C+2q\sqrt{3-q^2}\sqrt{2-p^2}V$	$0.1\left(3-q^2\right)p^2A+q^2C+0.9q\sqrt{\frac{3-q^2}{2}}pU$
$\left\|\mathbf{r}_1^p+\mathbf{r}_2^p-\mathbf{r}_3^p\right\|^2$	$\left(3-q^2\right)\left(2-p^2\right)B+q^2C-2q\sqrt{3-q^2}\sqrt{2-p^2}V$	$0.1\left(3-q^2\right)p^2A+q^2C-0.9q\sqrt{\frac{3-q^2}{2}}pU$
$\left\|\mathbf{r}_1^p-\mathbf{r}_2^p-\mathbf{r}_3^p\right\|^2$	$\left(3-q^2\right)p^2A+q^2C-2q\sqrt{3-q^2}pU$	$0.9\left(3-q^2\right)p^2A+q^2C-2.7q\sqrt{\frac{3-q^2}{2}}pU$
$\left\|\mathbf{r}_1^p-\mathbf{r}_2^p+\mathbf{r}_3^p\right\|^2$	$\left(3-q^2\right)p^2A+q^2C+2q\sqrt{3-q^2}pU$	$0.9\left(3-q^2\right)p^2A+q^2C+2.7q\sqrt{\frac{3-q^2}{2}}pU$

Table 2. Euclidean distance between received symbols

Table 3. Final result of q_{opt} for the proposed precoding $(k = A/B)$

Modulation	Case	q_{opt}
4-QAM	$1 \le k < 7$	$\max\left(\sqrt{\frac{12W^2}{C^2+4W^2}}, \sqrt{\frac{3(2-p^2)B}{C+(2-p^2)B}}\right)$
	$k \ge 7$	$\max\left(\sqrt{\frac{1.2p^2U^2}{C^2+0.4p^2U^2}}, \sqrt{\frac{0.3p^2A}{C+0.1p^2A}}\right)$
16-QAM	$\Delta < \frac{d_{\min}}{2}$	2.0
	$\frac{d_{\min}}{2} \le \Delta < \frac{d_{\min}}{\sqrt{2}}$	1.5
	$\frac{d_{\min}}{\sqrt{2}} \le \Delta < \sqrt{2}d_{\min}$	1
	$\Delta \ge \sqrt{2}d_{\min}$	0.6

for selection. Figure 2 shows that OSM-MHS provides about 8dB gains over the OSM at a BER of 10^{-4}

~~Figure 3 shows the BER performance of various systems with 16-QAM, which are similar to those of 4-QAM in Figure 2. We can see that only with 8 bits quantization we can achieve same performance as ARITH-BER. Also we present the simulation result of OSM-MHS to confirm the benefits of the $d_{\min}$ maximization. It shows that we can obtain about 5dB gains at a BER of 10^{-4} over the OSM~~

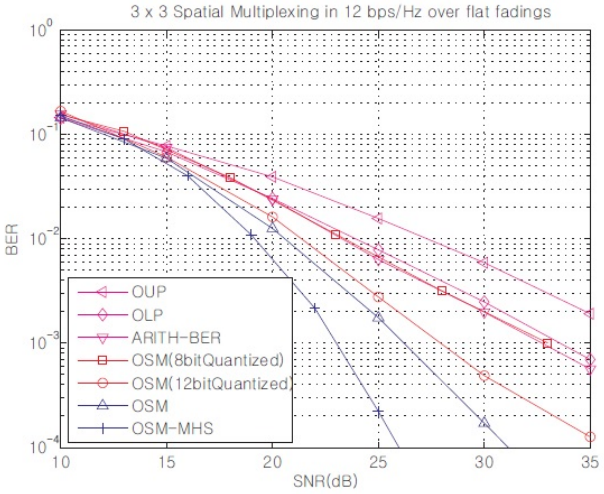

Figure 3. BER performance comparison of the proposed schemes with 16QAM

6. Conclusion

In this paper, we have presented a new efficient precoder design for closed-loop MIMO systems. The main objective of this work is the extension of the original OSM scheme to multiple data stream transmission. The essential advantage of the OSM is to maximize the system performance with low complexity in detection and computation. The proposed schemes may reduce the feedback information amount compared to the conventional SVD based schemes. Also, for the purpose of performance improvement, we have studied a criterion to choose a vector with the maximum height from the plane

spanned by the other two vectors. The simulation results confirm the efficiency of the OSM and the OSM-MHS scheme in practical situations.

7. Acknowledgement

This work was supported in part by National Research Foundation (NRF) of Korea funded by Korea Government (MSIP) under Grant NRF-2014R1A2A1A10075097 and in part by Korea National University of Transportation in 2015.

8. References

[1] G. J. Foschini and M. Gans, "On Limits of Wireless Communications in a Fading Environment when Using Multiple Antennas," *Wireless Personal Communications*, vol. 6, pp. 311–335, March 1998.
[2] I. E. Telatar, "Capacity of multi-antenna Gaussian channels," *Eur. Trans. Telecom.*, vol. 10, pp. 585–595, November 1999.
[3] G. G. Raleigh and J. M. Cioffi, "Spatio-Temporal Coding for Wireless Communication," *IEEE Transactions on Communications*, vol. 46, pp. 357–366, March 1998.
[4] H. Sampath, P. Stoica, and A. Paulraj, "Generalized Linear Precoder and Decoder Design for MIMO Channels Using the Weighted MMSE Criterion," *IEEE Transactions on Communications*, vol. 49, pp. 2198– 2206, December 2001.
[5] D. P. Palomar, J. M. Cioffi, and M. A. Lagunas, "Joint Tx-Rx Beamforming Design for Multicarrier MIMO Channels: A Unified Framework for Convex Optimization," *IEEE Transactions on Signal Processing*, vol. 51, pp. 2381–2401, September 2003.
[6] H. Lee, S.-H. Park, and I. Lee, "Orthogonalized Spatial Multiplexing for Closed-Loop MIMO Systems," *IEEE Transactions on Communications*, vol. 55, pp. 1044–1052, May 2007.
[7] Y.-T. Kim, H. Lee, S.-H. Park, and I. Lee, "Optimal Precoding for Orthogonalized Spatial Multiplexing in Closed-Loop MIMO Systems," *IEEE Journal on Selected Area in Communicaions*, vol. 26, pp. 1–11, Oct 2008.
[8] C. Song and I. Lee, "Orthogonalized Spatial Multiplexing for Rank-3 Transmission in Closed-loop MIMO Systems," *SK Telecommunications Review*, vol. 21, pp. 706–716, Aug 2011.